

## Limiting Angular Momenta for the Reactions of 45- to 180-MeV $^{12}\text{C}$ Projectiles with Al, Ti, Ni, and Cu

J. B. Natowitz, E. T. Chulick, and M. N. Namboodiri

*Department of Chemistry and Cyclotron Institute, Texas A&M University, College Station, Texas 77843*

(Received 19 July 1972)

Cross sections for complete fusion have been measured for the reactions of  $^{27}\text{Al}$ ,  $^{48}\text{Ti}$ , Cu, and Ni target nuclei with  $^{12}\text{C}$  projectiles accelerated by the Texas A&M variable-energy cyclotron. Both mica track detectors and solid-state detectors have been used to measure energy spectra, range distributions, and angular distributions for the recoiling product nuclei. The limiting angular momentum,  $J_{\text{crit}}$ , above which complete fusion does not occur is derived using a sharp cutoff model. This limiting angular momentum is found to increase slowly with excitation energy. Possible interpretations of this energy dependence are discussed.

### I. INTRODUCTION

The high probability for complete fusion of projectile and target in heavy-ion-induced nuclear reactions has made such reactions very useful in the synthesis of new isotopes and elements as well as in studies of the statistical properties of highly excited nuclei. Measurements of the complete-fusion cross sections provide information which should serve to characterize the initial properties of the excited product nuclei, making possible more reliable interpretations of the subsequent deexcitation processes.

In a previous paper<sup>1</sup> the available data on complete-fusion cross sections were found to be consistent within experimental errors with a simple sharp cutoff model. In that work, it appeared that there was, for each product nucleus, a fixed value of the angular momentum,  $J_{\text{crit}}$ , above which complete fusion did not occur. To explore further the question of the excitation-energy dependence of  $J_{\text{crit}}$ , we have performed another series of complete-fusion cross-section measurements. Complete-fusion cross sections have been measured for the reactions of 45- to 180-MeV  $^{12}\text{C}$  projectiles with  $^{27}\text{Al}$ ,  $^{48}\text{Ti}$ , Cu, and Ni target nuclei. These new measurements indicate a slow increase of  $J_{\text{crit}}$  with excitation energy.

### II. EXPERIMENTAL PROCEDURE

#### A. Experiments with Dielectric Track Detectors

In Fig. 1 we show a schematic diagram of the experimental geometry employed in most of the complete-fusion cross-section measurements reported here. The incident beam, focused into a spot of approximately 3 mm diam, passed through the target and was collected in a Faraday cup down-

stream from the target. Scattered projectiles were monitored with a solid-state detector placed behind a  $\frac{1}{16}$ -in.-diam collimator at  $20^\circ$  to the incident beam direction. Self-supporting targets of  $^{27}\text{Al}$  ( $123 \mu\text{g}/\text{cm}^2$ ),  $^{48}\text{Ti}$  ( $485 \mu\text{g}/\text{cm}^2$ ), Cu ( $262 \mu\text{g}/\text{cm}^2$ ), and Ni ( $202 \mu\text{g}/\text{cm}^2$ ) were used in this work. Each experiment consisted of two irradiations. First the ratio of scattered beam to integrated beam was determined in a run in which the target was in place but no mica detector was present. Then, with a mica detector<sup>2</sup> in place, the irradiation was repeated. In this way the elastic scattering of the projectiles could be directly related to the actual beam intensity for the purposes of cross-section calculations. For the lighter target elements at the higher projectile energies, the cross section for scattering was very small at  $20^\circ$ . However, light particles resulting from various nuclear reactions in the target were detected and could be used as a monitor, since only very low-energy-background pulses were observed in blank runs in which an empty target ring and mica detector were in place.

Following an exposure, the mica track detectors were etched in 48% HF at room temperature for 20 min. The detectors were then optically scanned at  $1250\times$  magnification. The criteria employed in the scanning operation have been discussed previously.<sup>1</sup> Basically, it is demanded that an acceptable track have perceptible length  $>0.5 \mu$  of mica and be oriented in the field of view so as to place the point of origin of the ionizing particle at the center of the irradiated target. The track length distribution must be symmetrical about some average length (which is less than the actual average range of recoiling products in the mica)<sup>3</sup> and the angular distributions must correspond to emission from the target in a narrow forward cone typical of compound-nucleus recoils.

Such criteria appear to discriminate very well against elastically scattered target nuclei (which should in fact be negligible at forward angles, as indicated by various heavy-ion-scattering experiments). These criteria also appear effective in discriminating against transfer reactions in which small pieces of the projectile are transferred to the target, since such reactions lead to much less momentum transfer than does complete fusion. Natural ionization thresholds of the mica help to prevent interferences from such processes. Reactions in which all but a small part of the projectile is transferred to the target nucleus would not be excluded from our scanning. However, these processes should have small cross sections. Any contribution from reactions of this type would increase the measured complete-fusion cross sections.

Cross sections for the production of heavy recoils satisfying the scanning criteria were obtained by numerical integration of the observed track densities.

#### B. Experiments with Solid-State Detectors

To measure the energy spectrum of the recoiling nuclei, we have used a detector stack consisting of an 8.4- $\mu$ -thick totally depleted surface-barrier detector ( $\Delta E$ ) in front of a 408- $\mu$  detector ( $E$ ). Since even an 8.4- $\mu$  detector is not thin enough to allow passage of all of the heavy-mass

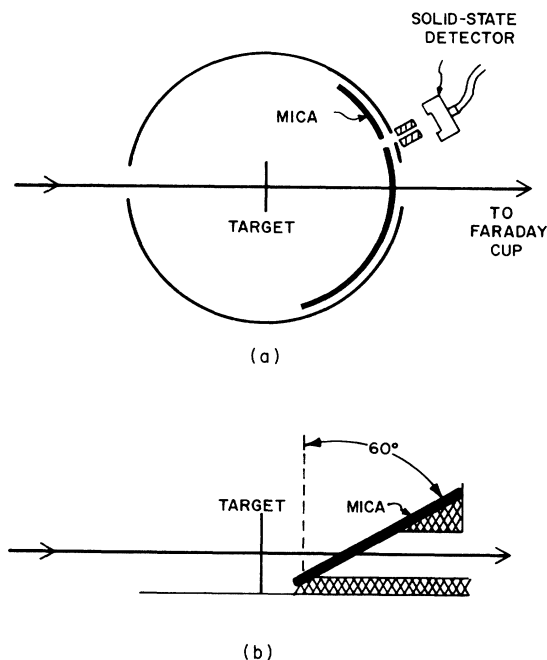


FIG. 1. (a), (b) Experimental geometry employed for the track detector experiments. Projectiles pass directly through the mica detectors.

products, we have performed two different experiments at each angle of observation.

First, data were taken in which we recorded only events occurring in coincidence in the two detectors. In such runs, the standard techniques of particle identification could be used to identify the events corresponding to the recoiling nuclei which had sufficient energy to pass through the first detector. The intensities of product nuclei as a function of atomic number were obtained.

In the second experiment, we recorded those events in the first detector which were in anti-coincidence with events in the second detector. Since the atomic number distribution of the product nuclei was known from the coincidence experiments, it was possible to choose an energy threshold<sup>4</sup> above which events must correspond to the stopping of nuclei with atomic numbers in the range of the product nuclei from the fusion reaction. In this way, many of the recoiling nuclei which were stopped in the first detector could be observed and their energy spectrum could be obtained.

Information obtained from a monitor detector placed at 20° to the initial beam direction was used to normalize the coincidence and anticoincidence data. Figure 2 shows the composite energy spectrum measured at 6° for the reaction 180 MeV  $^{12}\text{C} + ^{27}\text{Al}$ .

As may be seen, an extrapolation of the data was necessary at the low-energy end of the distribution. It is estimated that this extrapolation does not introduce an error greater than 3% into the determination of the cross section.

The energy distribution of the recoiling products was measured at 3° increments from 3 to 36°. Extrapolation of the angular distribution to 0° was

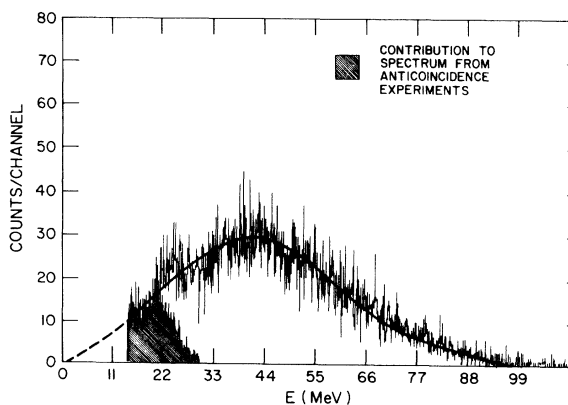


FIG. 2. Energy spectrum of recoiling product nuclei from the reaction  $^{27}\text{Al} + ^{12}\text{C}$  at 180 MeV. The data were taken at an angle of 6° to the beam. Both coincidence and anticoincidence data are shown.

TABLE I. Experimental complete-fusion cross sections. The estimated uncertainty for these cross sections is  $\pm 15\%$ .

$E$ (MeV)	$^{27}\text{Al}$		$^{48}\text{Ti}$		Target		Ni		Cu	
	$\sigma$ (b)	$\sigma_{\text{CF}}/\sigma_{\text{R}}$	$\sigma$ (b)	$\sigma_{\text{CF}}/\sigma_{\text{R}}$	$\sigma$ (b)	$\sigma_{\text{CF}}/\sigma_{\text{R}}$	$\sigma$ (b)	$\sigma_{\text{CF}}/\sigma_{\text{R}}$	$\sigma$ (b)	$\sigma_{\text{CF}}/\sigma_{\text{R}}$
180	0.834	0.478	1.20	0.590	1.16, 1.18	0.526, 0.539				
97.6	0.854	0.560	0.938	0.540	1.24	0.678	1.29	0.715		
96.5	1.00	0.654	...	...	1.05	0.581	1.07	0.592		
85.7	1.11	0.734	...	...	...	...	...	...		
81.0	1.15	0.768	0.943	0.580	1.217	0.710	0.886	0.517		
79.0	...	...	...	...	...	...	...	...		
63.8	1.14	0.754	...	...	0.956	0.675	1.11	0.789		
44.3	1.04	0.800	...	...	...	...	0.882	0.924		

accomplished by using as guides various angular distributions obtained with track detectors. The complete-fusion cross section at 180 MeV was obtained by integration of this angular distribution.

### III. EXPERIMENTAL RESULTS

In Table I are listed the complete-fusion cross sections measured in this work. Also shown are the ratios of these complete-fusion cross sections to the total-reaction cross sections calculated by Thomas.<sup>5</sup> ( $\text{Ni} + ^{12}\text{C}$  and  $\text{Ti} + ^{12}\text{C}$  total-reaction cross

sections were obtained from an interpolation of the cross sections in that reference.)

It is common practice to use optical-model calculations of the total-reaction cross sections for the comparison between measured cross sections and total-reaction cross sections. However, uncertainties as to appropriate parameters for this model for heavy-ion projectiles still exist. For example, in Fig. 3 we show, together with our measured complete-fusion-reaction cross sections for  $^{12}\text{C} + ^{27}\text{Al}$ , total-reaction cross sections calculated with two different sets of optical-model parameters.<sup>6,7</sup> The measured total-reaction cross sections of Wilkins and Igo<sup>8</sup> are in essential agreement with the Thomas calculations. A similar agreement is observed for  $^{12}\text{C} + \text{Cu}$  total-reaction cross sections.

The ratios of  $\sigma_{\text{CF}}/\sigma_{\text{R}}$  in Table I show a marked decrease from unity at the higher projectile energies, in agreement with previous experiments. It should be noted that the values for  $^{12}\text{C} + \text{Cu}$  are somewhat higher than those of Ref. 1, where it was suggested that the results presented for  $^{12}\text{C}$  induced reactions appeared systematically low, probably because the targets were too thick.

#### A. Interpretation

On the assumption that incomplete-fusion processes occur with the projectiles of higher impact parameter, we may use the sharp cutoff model to extract a limiting angular momentum,  $J_{\text{crit}}$ , which characterizes complete-fusion products.<sup>1</sup> In this model,  $P(L)$ , the distribution of orbital angular momenta which may lead to a nuclear reaction is assumed to be given by

$$P(L)dL = \frac{2L}{L_{\text{max}}^2} dL, \quad L \leq L_{\text{max}},$$

$$P(L)dL = 0, \quad L \geq L_{\text{max}}.$$

The intrinsic spins of the projectile and target are ignored so that the maximum possible angular

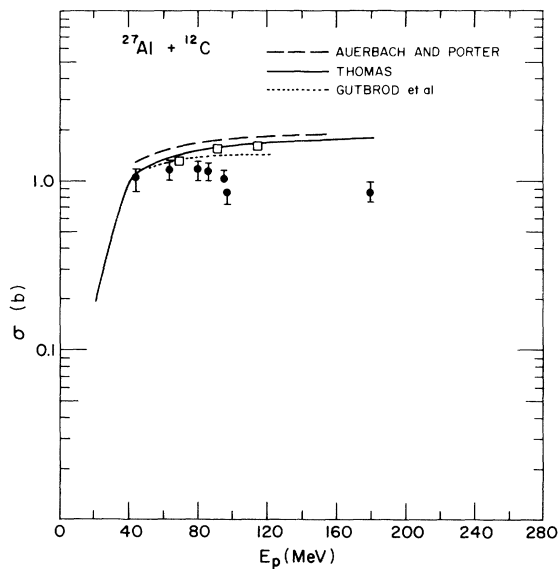


FIG. 3. Complete-fusion cross sections for the reaction of  $^{27}\text{Al}$  with  $^{12}\text{C}$ . The experimental data are indicated by the solid points. The solid line is the total reaction cross section calculated by Thomas (Ref. 5). Optical-model total-reaction cross sections calculated with parameters suggested by Auerbach and Porter (Ref. 6) and by Gutbrod, Yoshida, and Block (Ref. 7) are also shown. Open squares are the experimental total-reaction cross sections determined by Wilkins and Igo (Ref. 8).

momentum  $J_{\max} = L_{\max}$ . The actual angular momentum distribution of complete-fusion products is assumed to have the same functional form as the distribution of  $L$ , but to be limited by  $J_{\text{crit}}$  rather than by  $J_{\max}$ . Thus  $J_{\text{crit}} = (\sigma_{\text{CF}}/\sigma_{\text{R}})^{1/2} J_{\max}$ . It should be noted that only for cases in which there are very small contributions from incomplete-fusion processes would the value of  $J_{\text{crit}}$ , derived using the sharp cutoff model, differ from that derived using an optical-model angular momentum spectrum which corresponds to the same total-reaction cross section. In Figs. 4, 5, and 6, the derived values of  $J_{\text{crit}}$  are presented on a plot of excitation energy in the complete-fusion product nucleus versus angular momentum. Since Ni and Cu differ by only one atomic number, the data for these two targets have been plotted on the same figure. The variation of  $J_{\max}$  for production of each of the complete-fusion products, in the reactions indicated, is also shown.

Data from previous experiments of this type appeared to be consistent, within the experimental uncertainties of the measurements, with a single

limiting value of  $J_{\text{crit}}$  for each product nucleus. The present data, obtained over a wider range of excitation energy, do not correspond to a fixed value of  $J_{\text{crit}}$ . Instead the limiting angular momentum is found to increase with excitation energy, although not nearly as rapidly as the calculated values of  $J_{\max}$ .

#### IV. DISCUSSION

Several different approaches have been made to calculating an upper limit to the nuclear angular momentum which may be produced in a heavy-ion reaction.

For example, Kalinkin and Petkov<sup>9</sup> have considered the formation of an ellipsoidal nucleus during the collision of the target and projectile and derived a limiting angular momentum for the survival of such a nucleus. Using the same set of parameters as was employed in Ref. 1, we have calculated the limiting angular momenta for the cases presented in Figs. 4–6. Unlike the critical angular momenta derived from our experiments, the limiting angular momenta calculated in this

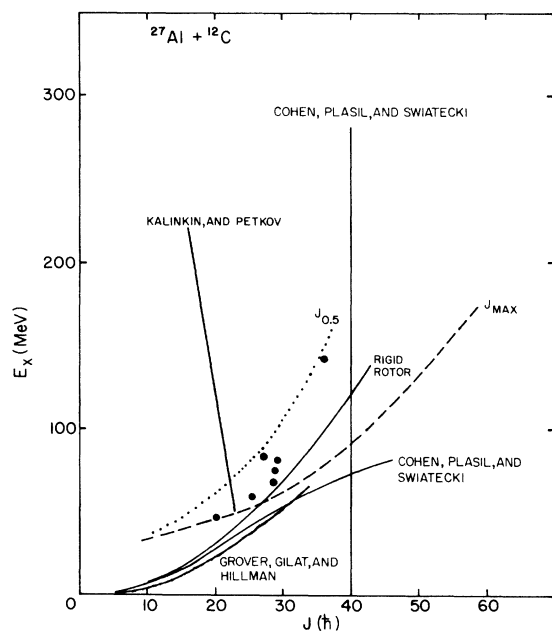


FIG. 4.  $J_{\text{crit}}$  as a function of excitation energy for  $^{39}\text{K}$  produced in the reaction  $^{27}\text{Al} + ^{12}\text{C}$ . Solid circles show values derived from the experimental data. The solid lines indicate various possible limits to the angular momentum in  $^{39}\text{K}$  (see text). The dashed line indicates for each excitation energy, the maximum angular momentum which can result from a fusion of  $^{12}\text{C}$  and  $^{27}\text{Al}$ . The dotted line corresponds to the maximum angular momentum which would result from fusion at an impact parameter equal to the sum of the half-density radii of the colliding nuclei (see text).

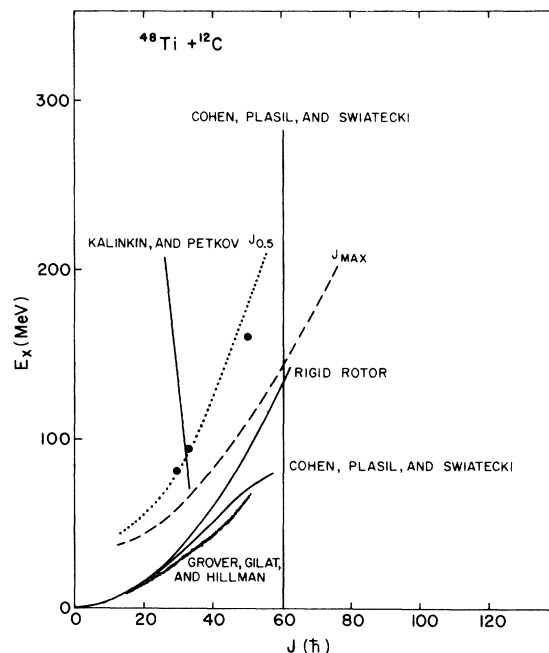


FIG. 5.  $J_{\text{crit}}$  as a function of excitation energy for  $^{39}\text{K}$  produced in the reaction  $^{48}\text{Ti} + ^{12}\text{C}$ . Solid circles show values derived from the experimental data. The solid lines indicate various possible limits to the angular momentum in  $^{60}\text{Ni}$  (see text). The dashed line indicates for each excitation energy, the maximum angular momentum which can result from a fusion of  $^{12}\text{C}$  and  $^{48}\text{Ti}$ . The dotted line corresponds to the maximum angular momentum which would result from fusion at an impact parameter equal to the sum of the half-density radii of the colliding nuclei (see text).

manner are seen to decrease with increasing excitation energy. A different choice of parameters could shift the location of the calculated lines, but the decrease with increasing excitation energy would persist.

Another possible interpretation of the limitation to complete-fusion processes could be that at the particular excitation energy attained in the product nucleus, there can be no levels with angular momenta higher than the limiting value. Projectile-target collisions which would have produced higher-angular-momentum states must therefore proceed through other reaction channels. We have calculated the energies of the "yrast" levels<sup>10</sup> (levels with maximum angular momentum at a particular excitation energy) in <sup>39</sup>K, <sup>60</sup>Ni, and <sup>75</sup>Br, in three different ways. The uppermost solid curves in Figs. 4, 5, and 6 are the yrast lines calculated assuming that the total excitation energy is manifested as rotational energy of a spherical nucleus with a moment of inertia equal to that of a rigid body. A radius parameter equal to 1.20 fm has been used.

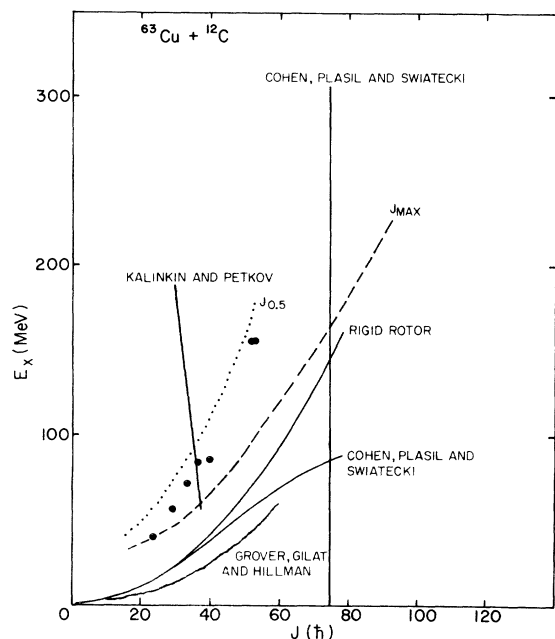


FIG. 6.  $J_{crit}$  as a function of excitation energy for <sup>75</sup>Br produced in the reaction <sup>63</sup>Cu + <sup>12</sup>C. Solid circles show values derived from the experimental data for both <sup>12</sup>C + Ni and <sup>12</sup>C + Cu reactions. The solid lines indicate various possible limits to the angular momentum in <sup>75</sup>Br (see text). The dashed line indicates for each excitation energy, the maximum angular momentum which can result from a fusion of <sup>12</sup>C and <sup>63</sup>Cu. The dotted line corresponds to the maximum angular momentum which would result from fusion at an impact parameter equal to the sum of the half-density radii of the colliding nuclei (see text).

The wavy curves in the figures represent the calculations of the yrast levels using YRASTGH,<sup>11</sup> a combinatorial calculation based on the single-particle model. The lower solid curves in the figures are the yrast lines calculated according to the liquid-drop-model picture of Cohen, Plasil, and Swiatecki,<sup>12</sup> in which the nuclear shape becomes increasingly nonspherical as the angular momentum increases.

At all excitation energies in <sup>60</sup>Ni and <sup>75</sup>Br, each of the three calculations leads to a yrast angular momentum which is higher than the maximum possible angular momentum which can be produced in the <sup>48</sup>Ti + <sup>12</sup>C and Cu + <sup>12</sup>C reactions. For the <sup>27</sup>Al + <sup>12</sup>C reaction, the rigid rotor calculation and the combinatorial calculation, both based on the assumption of a spherical nucleus, imply that the yrast limit would be encountered at  $\sim 25\hbar$  to  $35\hbar$ . In contrast, the liquid-drop-model calculation indicates that at all excitation energies, the maximum possible angular momentum resulting from the fusion of <sup>27</sup>Al with <sup>12</sup>C is lower than the angular momentum corresponding to the yrast limit.

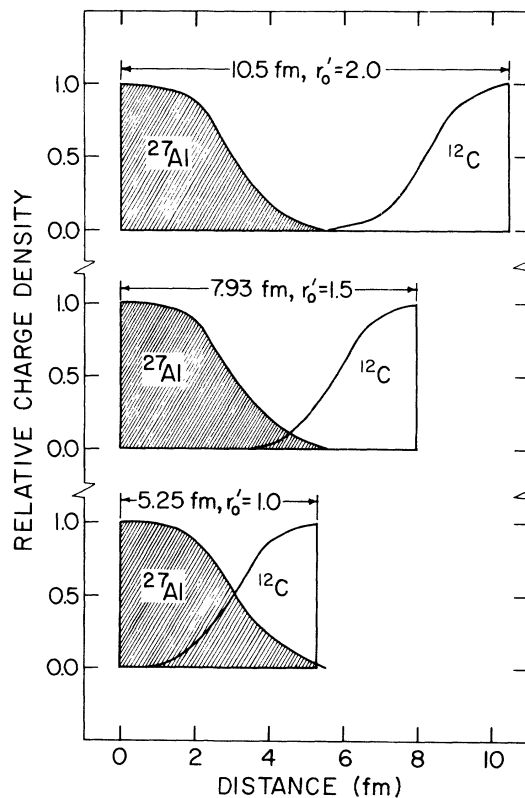


FIG. 7. Overlap of the nuclear charge densities of <sup>27</sup>Al and <sup>12</sup>C at three different impact parameters. "Effective" radius parameters  $r'_0$  are derived from the relationship  $r'_0(12^{1/3} + 27^{1/3}) = \text{impact parameter}$ .

The liquid-drop-model calculation does lead to the conclusion that the fission barrier in the compound nucleus decreases with increasing angular momentum. The angular momentum at which the fission barrier becomes equal to zero is the critical angular momentum for the system. This limit has a constant value independent of excitation energy. The solid vertical lines in Figs. 4, 5, and 6 indicate the calculated critical angular momentum<sup>12</sup> values for <sup>39</sup>K, <sup>60</sup>Ni, and <sup>75</sup>Br.

The critical angular momentum limits derived from our data should serve to characterize better the initial angular momentum distribution of compound nuclei produced in these reactions. However, in comparing these critical angular momenta with theoretical limits, we should not lose sight of the fact that there may be, particularly at higher projectile energies, a significant probability of non-fusion reactions which would occur even if there were no angular momentum limit in the nucleus. The effect of such peripheral reactions would be to cause the derived values of the angular momentum to remain lower than any actual nuclear limit. The actual limit might then be approached only at high projectile energies such that very high angular momenta can be produced at very low impact parameters, in which case the overlap between the two nuclear potentials is so strong that a fusion would almost certainly occur if there were no limit to the angular momentum of the product nucleus. For example, it is well known that measurements of both Coulomb barriers and total-reaction cross sections for heavy-ion reactions suggest a uniform density radius parameter  $r_0 \approx 1.5$  fm, significantly higher than the 1.2 to 1.3 fm derived from electron scattering experiments.<sup>13</sup> Such an interaction distance corresponds to nuclear reactions taking place when there is only slight overlap between the nuclear potentials of the interacting nuclei. This is shown in Fig. 7, where the overlap of the relative nuclear charge densities<sup>13</sup> for <sup>12</sup>C and <sup>27</sup>Al is shown for three different reaction impact parameters. Also indicated is the "effective" uniform density radius parameter,  $r'_0$ , which is derived from the relationship:

$$r'_0(A_p^{1/3} + A_t^{1/3}) = \text{impact parameter.}$$

We see then that  $r'_0 = 1.5$  fm corresponds to a situation in which the overlap occurs at a point where the nuclear densities have decreased to ~10% of the density at the center of the nucleus. At higher projectile energies, one expects that at this impact parameter the two nuclei might fuse into a compound nucleus only rarely; i.e., that reactions at the nuclear surface are predominantly transfer reactions.

Within the framework of the sharp cutoff model, we expect that at some impact parameter, fusion rapidly becomes the dominant process. We have made no attempt to fit the data exactly in order to extract a value of this impact parameter. However, for comparison with the data, we have plotted in Figs. 4, 5, and 6, the angular momenta for compound nuclei formed at impact parameters corresponding to the sum of the half-density radii of the two reacting nuclei. This condition is illustrated in Fig. 7 for the <sup>12</sup>C + <sup>27</sup>Al reaction. The experimental points are in rough agreement with the excitation-energy dependence indicated by that line.

It is possible that such an excitation energy dependence could continue until some other limitation, for example the angular momentum limit postulated by Cohen, Plasil, and Swiatecki, is encountered. Since, however, this limit corresponds to the point where the fission barrier has decreased to zero, it is suspected that fission becomes increasingly significant as a deexcitation process as the limit is approached.<sup>14</sup> In such a situation, our critical angular momenta, derived from the cross sections for production of nonfissioning compound nuclei, should remain less than the critical limit calculated from the liquid-drop model.

## V. CONCLUSIONS

The experimental complete-fusion cross sections indicate a limiting angular momentum,  $J_{\text{crit}}$ , which increases slowly with excitation energy in the compound nucleus in contrast to the calculations of Kalinkin and Petkov. The yrast-level calculations for a spherical <sup>39</sup>K nucleus suggest the possibility of a limitation to the fusion process because of the nonavailability of levels of high angular momentum. However, the liquid-drop-model calculations indicate that such a limitation need not exist because the nuclear shape is not spherical. Relaxation to a spherical nucleus necessitates the dissipation of considerable angular momentum which might be accomplished in some cases by multiple emission of  $\alpha$  particles or heavier fragments and might therefore result in a fusion event which is not detected as such in our experiments. In such a situation, the yrast levels of the residual nucleus formed in the deexcitation step could appear to limit the fusion process. However, the measurements for the <sup>60</sup>Ni and <sup>75</sup>Br nuclei indicate the same qualitative variation of  $J_{\text{crit}}$  as is observed for <sup>39</sup>K even though the calculated yrast lines do not suggest an yrast limitation to complete fusion. In view of this fact, an argument for yrast limitation in <sup>39</sup>K would not appear justified.

Earlier experiments, most of them done over a more limited range of compound-nucleus excita-

tion energies, had suggested that a constant limiting angular momentum, as suggested by the liquid-drop model, had been observed. In view of the present results, it would appear that such is not the case. However, in the reaction  $^{12}\text{C} + ^{27}\text{Al}$ , the limiting angular momentum of  $36\hbar$  at 180-MeV projectile energy is close to the  $40\hbar$  limit calculated for  $^{39}\text{K}$  and should projectiles of suitable energy become available, it would obviously be of considerable interest to perform similar experiments at higher excitation energies.

## ACKNOWLEDGMENTS

We particularly wish to thank Dr. R. Kenefick, Dr. Phil Chamberlin, G. DeHaven, and W. Walterscheid for their work in obtaining the heavy-ion beams. Our thanks also to Mrs. Ona Pridgeon, who patiently scanned all of the track detectors and Miss C. Schnatterly, who assisted with the data reduction. This research was supported by the U. S. Atomic Energy Commission and The Robert A. Welch Foundation.

- <sup>1</sup>J. B. Natowitz, Phys. Rev. C 1, 623 (1970).  
<sup>2</sup>R. L. Fleischer, P. B. Price, and R. M. Walker, Ann. Rev. Nucl. Sci. 15, 1 (1965).  
<sup>3</sup>H. Blok, F. M. Kiely, and B. D. Pate, Nucl. Instr. Methods 100, 403 (1972).  
<sup>4</sup>L. C. Northcliffe and R. Schilling, Nucl. Data 7, 233 (1970).  
<sup>5</sup>T. D. Thomas, Phys. Rev. 116, 703 (1959).  
<sup>6</sup>E. H. Auerbach and C. E. Porter, in *Proceedings of the Third Conference on Reactions between Complex Nuclei, Pacific Grove, California* (Univ. California Press, Berkeley, 1963), p. 19.  
<sup>7</sup>H. H. Gutbrod, H. Yoshida, and R. Bock, Nucl. Phys. A165, 240 (1971).  
<sup>8</sup>B. Wilkins and G. Igo, in *Proceedings of the Third Conference on Reactions between Complex Nuclei, Pacific Grove, California* (see Ref. 6), p. 241.  
<sup>9</sup>B. N. Kalinkin and I. Z. Petkov, Acta Phys. Polon. 25, 265 (1964).  
<sup>10</sup>J. R. Grover, Phys. Rev. 157, 832 (1967).  
<sup>11</sup>M. Hillman and J. R. Grover, Phys. Rev. 183, 1303 (1969).  
<sup>12</sup>S. Cohen, F. Plasil, and W. J. Swiatecki, in *Proceedings of the Third Conference on Reactions between Complex Nuclei, Pacific Grove, California* (see Ref. 6), p. 325; F. Plasil, in Proceedings of the European Conference on Nuclear Physics, Aix-en-Provence, France, 1972 (to be published).  
<sup>13</sup>R. Hofstadter, Rev. Mod. Phys. 28, 214 (1956).  
<sup>14</sup>M. Blann and F. Plasil, Phys. Rev. Letters 29, 303 (1972).

## $^{91}\text{Zr}(p, t)$ Reaction and the Level Structure of $^{89}\text{Zr}^\dagger$

J. B. Ball

Oak Ridge National Laboratory, Oak Ridge, Tennessee 37830

(Received 10 August 1972)

The  $^{91}\text{Zr}(p, t)$  reaction has been studied at a proton energy of 31 MeV. Tritons were detected in a magnetic spectrograph yielding a resolution of 18 keV. Angular distributions for levels up to 2.75 MeV of excitation in  $^{89}\text{Zr}$  are compared to two-nucleon-transfer distorted-wave Born-approximation calculations and analyzed in terms of the mixed  $L$  transfers allowed from a nonzero-spin target. Two types of neutron configurations are observed to be populated in  $^{89}\text{Zr}$  by this reaction: single-hole states and one-particle, two-hole states.

## I. INTRODUCTION

Much of the existing data on two-neutron-transfer reactions such as  $(p, t)$  and  $(t, p)$  are concentrated on studies with even-target nuclei. One reason for this is the simplification introduced by the selection rules governing these reactions.<sup>1</sup> For a  $(p, t)$  or  $(t, p)$  reaction from a  $0^+$  initial state, only the natural-parity states of the final nucleus

will be populated in the direct one-step transfer process. In addition, each final state will be populated with a unique  $L$ -transfer value. Thus the determination of the  $L$  value for a given final-state angular distribution gives directly both the spin and parity of the level observed.

The situation for  $(p, t)$  or  $(t, p)$  from nonzero-spin targets will usually be more complex. In general, more than one  $L$  transfer will contribute

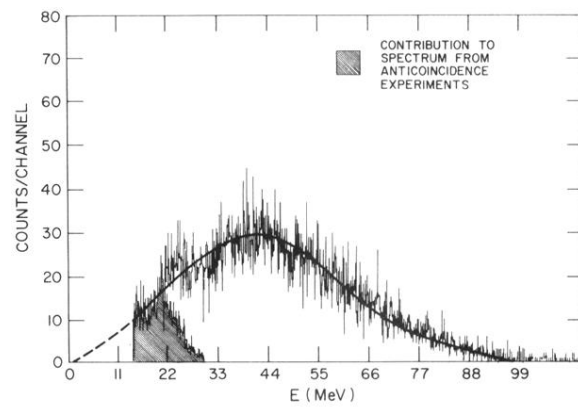


FIG. 2. Energy spectrum of recoiling product nuclei from the reaction  $^{27}\text{Al} + ^{12}\text{C}$  at 180 MeV. The data were taken at an angle of  $6^\circ$  to the beam. Both coincidence and anticoincidence data are shown.